Limits to Genomic Divergence Under Sexually Antagonistic Selection

Katja R. Kasimatis, Peter L. Ralph, and Patrick C. Phillips

Institute of Ecology and Evolution, 5289 University of Oregon, University of Oregon, Eugene, OR 97403

Running Title: Sex-Specific Genomic Divergence

Keywords: antagonistic selection, sexual conflict, male-female divergence, intersexual F_{ST}, genetic load

Corresponding Author: Katja Kasimatis
Institute of Ecology and Evolution, 5289 University of Oregon, Eugene, OR 97403
(541) 346-0519
kkasimat@uoregon.edu

Abstract

Since the autosomal genome is shared between the sexes, sex-specific fitness optima present an evolutionary challenge. While sexually antagonistic selection might favor different alleles within males and females, segregation randomly reassorts alleles at autosomal loci between sexes each generation. This process of homogenization during transmission thus prevents between-sex allelic divergence generated by sexually antagonistic selection from accumulating across multiple generations. However, recent empirical studies have reported high male-female F_{ST} statistics. Here, we use a population genetic model to evaluate whether these observations could plausibly be produced by sexually antagonistic selection. To do this, we use both a single-locus model with nonrandom mate choice, and individual-based simulations to study the relationship between strength of selection, degree of between-sex divergence, and the associated genetic load. We show that selection must be exceptionally strong to create measurable divergence between the sexes and that the decrease in population fitness due to this process is correspondingly high. Individual-based simulations with selection genome-wide recapitulate these patterns and indicate that small sample sizes and sampling variance can easily generate substantial male-female divergence. We therefore conclude that caution should be taken when interpreting autosomal allelic divergence between the sexes.

Introduction

Females and males use largely the same genome to produce distinct phenotypes and behaviors. This ubiquitous phenomenon requires an association between dimorphic phenotypes and their sexual environment [Kasimatis et al., 2017, Mank, 2017a]. Genes residing on a sex chromosome have a physical link to sex determination. Particularly, on heteromorphic sex chromosomes, the lack of recombination allows for selection to act in a sex-specific manner to optimize beneficial genes within each sex [Rice, 1984, 1987, Charlesworth and Charlesworth, 1980]. Conversely, the shared genetic basis of autosomal genes prevents such sex-specific optimization of fitness. When autosomal-based traits have different optimal fitness values in each sex, then selection acts in a sexually antagonistic manner to push females and males in opposing directions in phenotype space [Rice and Holland, 1997, Bonduriansky and Chenoweth, 2009]. However, recombination and

meiotic segregation uncouple beneficial alleles from their sexual environment every generation, preventing the resolution of antagonism via the creation of separate female and male genomic pools. This homogenization process tethers together the evolutionary responses of the sexes and creates an inherent intersexual genomic conflict [as reviewed in Kasimatis et al., 2017].

Identifying sexually antagonistic loci – particularly using reverse genomics approaches – has proved challenging. Initial studies calculated differentation between females and males using Wright's fixation index (F_{ST}), and interpreted high values as evidence of sexually antagonistic selection. Empirical data from multiple taxonomic groups [Lucotte et al., 2016, Flanagan and Jones, 2017, Wright et al., 2018, Cheng and Kirkpatrick, 2016, Dutoit et al., 2018] suggest that hundreds to thousands of SNPs have a significant male-female autosomal divergence in many cases exceeding $F_{ST} = 0.01$ [Lucotte et al., 2016, Wright et al., 2018] and even approaching $F_{ST} = 0.2$ [Flanagan and Jones, 2017]. Taken at face value, both the number of sexually antagonistic alleles and the degree of divergence are striking. However, these results are difficult to evaluate as they suggest that there must be quite strong selection within each sex to drive such high divergence within a generation.

Several different processes could in principle generate divergence (or apparent divergence) between the sexes. First, sex biases in chromosome segregation through associations with the sex determining region could distort allele frequencies between the sexes. Over time, this segregation distortion can contribute to the generation of neo-sex chromosomes [Jaenike, 2003, Kozielska et al., 2010] – particularly heteromorphic sex chromosomes – leading to sex-specific differentiation in the trivial sense that the locus is completely absent in one sex. Second, gametic selection resulting in a sex-specific fertilization bias could also distort allele frequencies [Joseph and Kirkpatrick, 2004]. Both of these processes occur during the gametic phase of the lifecycle and have long been recognized for their potential ability to distort segregation ratios within the sexes [reviewed in Immler and Otto, 2018]. In contrast, sexually antagonistic viability selection that occurs post-fertilization is a fundamentally different mechanism because there is no direct co-segregation of sex with the alleles under selection. Previous work on sexually antagonistic viability selection has largely focused on its potential role in maintaining genetic variation due to the sex-specific pleiotropic effects of the locus. In particular, Kidwell et al. [1977] laid out a framework for analyzing sexual antagonism that has widely been used in the field [Arnqvist, 2011, Connallon et al., 2010, Connallon and Clark, 2011, Patten and Haig, 2009, Fry, 2010]. A little appreciated feature of the Kidwell model is that it tracks allele frequencies (rather than diploid genotype frequencies) in adults from each generation to the next. Although the model incorporates diploid selection, this sampling paradigm is sufficient because the "random union of gametes" model of mating only requires allele frequencies to generate diploid genotype frequencies in the next generation. However, this model simplification prevents the inclusion of other models of mating, such as assortative mating among genotypes.

In this paper, we will first build a model of sexually antagonistic viability selection, segregation, and transmission, extending the model of Kidwell et al. [1977] to include assortative mating. We use this model to evaluate how much between-sex differentiation is produced across a range of selection, dominance, and assortative mating parameters. Second, we use these results to evaluate the claims that the observed between-sex allelic differentiation is cuased by sexually antagonistic viability selection. We then use simulation to test the conclusions of our deterministic model, as well as the role of sampling variance in generating loci with high between-sex differentiation. Both our single locus model and individual-based simulations with antagonistic loci distributed genome-wide indicate that antagonistic selection must be remarkably strong to produce non-negligible divergence between the sexes. Instead, simulations indicate that sampling variance is much more likely to account for extreme between-sex divergence and must therefore be explicitly included in any analyses of putative signatures of male-female divergence.

Methods

Model

Consider an autosomal locus at which are found two alleles: one male-beneficial (A_1) and one female-beneficial (A_2). Sexual antagonism results in a fitness cost to individuals carrying the allele favored in the other sex [Kidwell et al., 1977, Bodmer, 1965]. Our life cycle is shown in figure 1. Each generation begins with zygotic frequencies equal in each sex, but then genotype-dependent survival results in different genotype frequencies in each sex at time of mating. The relative fitnesses of genotypes A_1A_1, A_1A_2, and A_2A_2 in females are $1 :: 1 - h_f s_f :: 1 - s_f$, where s_f is the cost of a female having the male-favorable allele and h_f is the dominance coefficient in females. Writing the frequencies of the three genotypes in zygotes as $p_{11}(t)$, $p_{12}(t)$, and $p_{22}(t)$ at the start of generation t, the genotype frequencies in females after selection will then be proportional to $p_{11}(t)$, $p_{12}(t)(1 - h_f s_f)$, and $p_{22}(t)(1 - s_f)$, respectively. Similarly, the relative fitnesses of the genotypes A_1A_1, A_1A_2, and A_2A_2 in males are $1 - s_m :: 1 - h_m s_m :: 1$, and the genotype frequencies in males after selection are proportional to $p_{11}(t)(1 - s_m)$, $p_{12}(t)(1 - h_m s_m)$, and $p_{22}(t)$, respectively.

Therefore, the frequency of the female-beneficial allele in females post-selection, which we denote $p_f(t)$, is

$$p_f(t) = \frac{p_{11}(t) + \frac{1}{2}p_{12}(t)(1 - h_f s_f)}{p_{11}(t) + p_{12}(t)(1 - h_f s_f) + p_{22}(t)(1 - s_f)}. \tag{1}$$

The same quantity for males is:

$$p_m(t) = \frac{p_{11}(t)(1 - s_m) + \frac{1}{2}p_{12}(t)(1 - h_m s_m)}{p_{11}(t)(1 - s_m) + p_{12}(t)(1 - h_m s_m) + p_{22}(t)}. \tag{2}$$

In a deterministic model of non-overlapping generations without gamete-specific selection, the genotype frequencies in the next generation are determined by the frequency of gametes joining from each of the nine possible mating combinations weighted according to mate choice. We parameterize mate choice using a matrix whose rows are indexed by male genotypes and columns by female genotypes, such that M_{ij} is the frequency of pairings of male genotype i with female genotype j relative to that expected under random mating. We focus on three common mating scenarios by structuring the mate choice matrix as:

$$\mathbf{M} = \begin{bmatrix} m_1 & m_2 & m_3 \\ m_2 & m_1 & m_2 \\ m_3 & m_2 & m_1 \end{bmatrix}.$$

Under random mating, each pairing occurs with equal likelihood ($m_1 = m_2 = m_3$). Positive assortative mating by genotype occurs when females and males with the same genotype mate more frequently than those with different genotypes ($m_1 > m_2 = m_3$). Conversely, disassortative mating by genotype – or positive assortative mating by fitness – occurs when A_1A_1 individuals mate with A_2A_2 individuals ($m_1 = m_2 < m_3$).

The genotype frequencies in the next generation can be concisely calculated with some matrix algebra. Let $\mathbf{w_f} = (1, 1-h_f s_f, 1-s_m)$ and $\mathbf{w_m} = (1-s_m, 1-h_m s_m, 1)$ be the vectors of relative fitnesses in females and males respectively. Then, define the 3×3 matrix of fitness-weighted mate pairings, $\mathbf{F}$, so that for each pair of genotypes a and b, the entry $\mathbf{F}_{ab} = w_m(a)M_{ab}w_f(b)$. In other words, $\mathbf{F} = \mathrm{diag}(w_m)M\,\mathrm{diag}(w_f)$, where $\mathrm{diag}(w_m)$ denotes the matrix with $\mathbf{w_m}$ on the diagonal and zeros elsewhere. Finally, define $\beta = \mathrm{diag}(1, 1/2, 0)$ and $\gamma = \mathrm{diag}(0, 1/2, 1)$. Then, the vector of frequencies of each genotype among zygotes (before selection) in the next generation can be calculated using the current frequencies as a weighted sum over possible mating pairs:

$$\begin{aligned} p_{11}(t+1) &= \frac{\mathbf{p(t)}^\mathbf{T}\beta\mathbf{F}\beta\mathbf{p(t)}}{\mathbf{p(t)}^\mathbf{T}\mathbf{F}\mathbf{p(t)}} \\ p_{22}(t+1) &= \frac{\mathbf{p(t)}^\mathbf{T}\gamma\mathbf{F}\gamma\mathbf{p(t)}}{\mathbf{p(t)}^\mathbf{T}\mathbf{F}\mathbf{p(t)}} \\ p_{12}(t+1) &= 1 - p_{11}(t+1) - p_{22}(t+1). \end{aligned} \tag{3}$$

Here, $\mathbf{p(t)} = (p_{11}(t), p_{12}(t), p_{22}(t))$ is the row vector of genotype frequencies and $\mathbf{p(t)}^T$ is its transpose. This set of equations can be derived by noting that the relative frequencies of A_1A_1, A_1A_2, and A_2A_2 genotypes produced in the next generation are $\mathbf{p(t)}^T\beta\mathbf{F}\beta\mathbf{p(t)}$, $\mathbf{p(t)}^T(\beta\mathbf{F}\gamma+\gamma\mathbf{F}\beta)\mathbf{p(t)}$, and $\mathbf{p(t)}^T\gamma\mathbf{F}\gamma\mathbf{p(t)}$, respectively; since $\beta + \gamma = I$, the identity matrix, these sum to $\mathbf{p(t)^T F p(t)}$, the denominator in equations (3).

We then used Mathematica v11.1.1.0 (Wolfram Research, Inc.) to find the equilibria of this system and determine stability of those equilibria. The complete notebook is provided in File S1.

Within-generation statistics

Sex-specific viability selection creates differences in allele frequencies between the sexes each generation. We can therefore quantify the effects of sexually antagonistic selection using the male-female F_{ST} statistic, which we calculate as the squared difference in allele frequencies between sexes, normalized by the total heterozygosity across sexes [Cheng and Kirkpatrick, 2016, Wright, 1951]:

$$F_{ST} = \frac{(p_m - p_f)^2}{4(p(t)_{11} + p(t)_{12}/2)(p(t)_{22} + p(t)_{12}/2)}. \tag{4}$$

Sex-specific selection creates divergence between the sexes by increasing the frequency of the beneficial allele in each sex. Therefore, at the population level, this opposing action of section skews genotype frequencies away from Hardy-Weinberg equilibrium. The degree of inbreeding within the population due to sex-specific effects can be quantified using Wright's F_{IS} statistic [Wright, 1951]:

$$F_{IS} = \frac{p(t)_{12}}{2(p(t)_{11} + p(t)_{12}/2)(p(t)_{22} + p(t)_{12}/2)} - 1.$$

A population fitness cost due to sexual antagonism (i.e., genetic load), is generated each generation. Within each sex, the genetic load is the difference between the maximum possible fitness and the mean fitness [Haldane, 1957, 1937]. The population's average genetic load (L) is the average of the loads for each sex (assuming an equal sex ratio), which is given by:

$$L = 1 - \frac{\bar{w}_m + \bar{w}_f}{2}, \tag{5}$$

where $\bar{w}_m = p_{11}(t)(1 - s_m) + p_{12}(t)(1 - h_m s_m) + p_{22}(t)$ and $\bar{w}_f = p_{11}(t) + p_{12}(t)(1 - h_f s_f) + p_{22}(t)(1 - s_f)$.

Simulations

We used R [R Core Team, 2018] (File S2) to simulate allele frequency dynamics at a single locus in a population subject to selection and drift. During viability selection each generation, each individual survived with probability equal to their (sex- and genotype-dependant) fitness. Then, the genotype frequencies within each sex were multiplied to give the matrix of relative frequencies of possible mating pairs, which was further weighted by the mate choice matrix. To generate the next generation, a fixed number of mating pairs are sampled from this distribution, and offspring are produced by random choice of parental alleles.

We also implemented simulations with sexually antagonistic selection acting at many loci, genome-wide with SLiM v3.1, an evolution simulation framework [Haller and Messer, 2019] (recipes in File S3). Individuals each had a genome of 100 Mb, a uniform recombination rate of 10^{-8}, and a mutation rate of 10^{-10}. All mutations are sexually antagonistic (we do not simulate neutral variation): each new mutations was beneficial in a randomly chosen sex and detrimental in the other, with selection coefficients drawn independently for each sex from a Gaussian distribution with mean zero and standard deviation 0.01. Each mutation also had dominance coefficients drawn independently for each sex from a uniform distribution between 0 and 1. The model had overlapping generations: each time step, first viability selection occurred (with probability of survival equal to fitness), followed by reproduction by random mating. The number of new offspring was chosen so that the population size fluctuated around 10,000 diploids, and simulations were run for 1,000

time steps. For a neutral comparison, we also simulated from the same scenario but with no fitness effects. We ran 25 independent simulations of each scenario (i.e., neutral and sexually antagonistic).

After the final generation, genetic load and male-female F_{ST} at each locus were calculated. F_{ST} values were calculated both using all individuals within the population as well as using smaller subsamples of 100 individuals and 50 individuals (equal numbers of each sex). Subsample sizes were chosen to reflect sample sizes currently used in the literature.

Data accessibility

The model equations, equilibrium analyses, and stability analyses are given in the Mathematica notebook in File S1. The single locus simulations and SLiM statistical analyses are given in File S2. The SLiM code and simulation data are available in Files S3-S5. Supplemental material is available at the Genetics Figshare archive: XXX.

Results

We first examine the conditions under which our model supports a stable polymorphism, and then examine the degree of between-sex divergence and genetic load expected under both equilibrium and non-equilibrium (selective sweep) conditions. Finally, we verify these results using simulations, which also provide an opportunity to explore the effects of statistical sampling on inferences of sex-specific differentiation from genomic samples.

Transmission dynamics at a sexually antagonistic locus

Maintenance of polymorphism requires symmetric selection between the sexes under random mating: We will quantify the strength and degree of asymmetry between the sex-specific allelic effects using the overall strength (s) and the ratio of selection coefficients (α), so that $s_m = s$ and $s_f = \alpha s$. The full solution for the maintenance of polymorphism under arbitrary patterns of dominance can be solved by setting $p(t+1) = p(t)$ in the recursion equations above (Equations (3); File S1). Under general conditions, this system yields a fifth-order polynomial that does not readily generate a closed form solution in symbolic form, although the equilibria can be easily found numerically. Symbolic solutions are possible under some specific conditions.

Assuming random mating and additivity of allelic effects ($h_m = h_f = 0.5$), the frequency of the A_1 allele at equilibrium (denoted $\hat{p}_{A1}$) can be expressed in terms of the strength of selection and asymmetry in selection:

$$\hat{p}_{A1} = \frac{1}{2} - \frac{1-\alpha}{2s\alpha}. \tag{6}$$

When selection is equally antagonistic across the sexes, an equilibrium frequency of $\hat{p}_{A1} = 0.5$ is always predicted. This theoretical solution is well supported by the stochastic simulations as well (Fig. 2A-B). The bounds on the non-trivial equilibrium frequency can be found by setting $\hat{p}_{A1}$ to zero or one. By solving these equations for α in terms of the strength of selection (s), we find that for the equilibrium to be stable, α and s must satisfy the condition:

$$\frac{1}{1+s} < \alpha < \frac{1}{1-s}. \tag{7}$$

These bounds can also be found by calculating the Jacobian matrix for the full set of transition equations (File S1) and agree with those identified by Kidwell et al. [1977]. In general, the equilibrium conditions describe an expanding envelope in parameter space that allows more asymmetry in the pattern of antagonistic selection as the absolute strength of selection increases (Fig. 3A & B). To a first order approximation in s, equation (7) shows that the equilibrium is stable only if asymmetry is not larger than the strength of

selection, such that $|\alpha - 1| < s$, as shown in Fig. 3A. Thus, when selection is weak or moderate, the maintenance of a polymorphism requires approximately equal selection between the sexes. However, the permissible degree of asymmetry increases with the strength of selection (Fig. 3B). For example, when $s \geq 0.4$ a stable polymorphism can be maintained so long as the asymmetry in fitness ($|1 - \alpha|$) is less than 50%. Selection coefficients of this magnitude mean mortality rates of 40% or higher each generation due to a single incorrect sexually antagonistic allele, which seems biologically implausible. Therefore, under additivity, any stable antagonistic polymorphisms must have approximately equal fitness effects in the two sexes, while less balanced antagonistic loci will quickly be fixed or lost.

On the other hand, if dominance is allowed to vary between the sexes but selection is equally antagonistic across the sexes ($\alpha = 1$), there is always a single real, non-trivial equilibrium (Fig. 3C), whose stability depends on the sum of the dominance coefficients between the sexes. When $h_m + h_f \leq 1$ the equilibrium is stable (File S1). This stability boundary makes sense as the mean fitness of homozygous individuals is lower than that of heterozygous individuals (assuming equal sex ratios):

$$1 - \frac{s}{2} \leq 1 - \frac{s(h_m + h_f)}{2}.$$

In other words, the equilibrium remains stable if the deleterious effects of dominance in one sex do not outweigh the benefits in the other sex. Interestingly, weak selection at a locus with sex-beneficial dominance ($h_m = h_f = 0$) can be more maintain a stable polymorphism despite greater asymmetry in selection than can an additive model (File S1). This expansion of the stability region is likely a result of heterozygotes being shielded from antagonistic selection and suggests that modifying dominance can act to maintain sexual antagonism at a locus. Conversely, when $1 < h_m + h_f \leq 2$, dominance favors the deleterious allele in each sex, pushing the population to an unstable state and leading to the fixation of the less costly allele. Allowing for asymmetry in the strength of selection narrows the equilibrium space and reduces the range of dominance coefficients resulting in stability (Fig. 3D).

Assortative mating by fitness expands the polymorphism space: Under positive assortative mating by fitness, high fitness matings occur between disparate genotypes and therefore produces an excess of heterozygotes each generation. Under this mating dynamic (with $m_3 > m_2 = m_1$), up to three real non-trivial equilibria can exist depending on the selection and dominance parameters (File S1). However, as with random mating, at most one equilibrium is stable. When selection is symmetrically antagonistic across the sexes ($\alpha = 1$), an A_1 allele frequency of approximately 0.5 is always predicted, regardless of dominance. This prediction is borne out by the single locus simulation results, which further show that assortative mating by fitness tends to make the stable equilibrium more robust to the effects of genetic drift (Fig. 2C). Increasing the asymmetry of selection can introduce an additional unstable equilibrium, and increasing the strength of sex-deleterious dominance (towards $h_m = h_f = 1$) can introduce a second unstable equilibrium (File S1). These theoretical predictions agree with previous simulations of assortative mating [Arnqvist, 2011]. As with random mating, the relationship between the strength and asymmetry in selection is the critical factor in determining when equilibria are stable. Specifically, when the asymmetry in selection is sufficiently large, fixation of the more favored allele is expected. Fixation only tends to occur under unrealistically large viability costs, however, and so the predominant outcome of assortative mating by fitness is the maintenance of heterozygotes and an expansion of the equilibrium space relative to random mating.

Assortative mating by genotype leads to fixation: In contrast to assortative mating by fitness, if assortative mating is by genotype ($m_1 > m_2 = m_3$), there is only a single non-trivial equilibrium (File S1). This equilibrium is always unstable, regardless of dominance, as shown by the leading eigenvalue of the Jacobian matrix. Fig. 2D shows allele frequency trajectories that start at this unstable equilibrium rapidly go to loss or fixation (with the choice determined by random genetic drift). Thus, these mating dynamics shrink the equilibrium space and lead to the loss of the weaker antagonistic allele.

Male-female divergence is exceptionally low

A number of studies have observed high mean male-female divergences (measured by F_{ST}). For instance, Dutoit et al. [2018] found a mean male-female $F_{ST} = 0.0016$ across genes with male-biased expression in a sample of 43 flycatchers of each sex. Wright et al. [2018] found a larger average male-female F_{ST} value of 0.03 across sex-biased genes in transcriptomes of 11 male and four female Trinidadian guppies. Simliarly, Flanagan and Jones [2017] identified 473 genome-wide outliers having male-female F_{ST} values above roughly 0.05 in a RADseq study of 171 male and 57 female gulf pipefish. Finally, Lucotte et al. [2016] found an average male-female F_{ST} of 0.067 across autosomal SNPs in the human HAPMAP data that showed significant nonzero male-female F_{ST} in all 11 populations (with around 100 samples of both sexes per population). Our previous work showed that selection within a single generation at an additive locus must be strong to generate a male-female $F_{ST} > 0.01$ [Kasimatis et al., 2017]. The model we study here allows us to estimate the strength of antagonistic selection required to produce male-female F_{ST} values as large as these, both at stably polymorphic loci and at loci undergoing a selective sweep.

When selection and dominance coefficients are chosen such that a stable equilibrium is maintained, divergence between the sexes tends to be exceptionally low (Fig. 4A). For example, a 10% viability cost ($s = 0.1$) results in a between-sex F_{ST} value of 0.0007 at equilibrium (assuming an additive locus and random mating). An equilibrium male-female F_{ST} value of 0.0016 (as in flycatchers) requires at least a 15% viability cost within each sex ($s = 0.15$, $\alpha = 1$). To produce equilibrium F_{ST} values an order of magnitude larger (as reported for the largest loci in the other taxa) requires a 30-65% viability cost ($s = 0.30 - 0.65$, $\alpha = 0.8 - 2.0$). For these values to be a produce of viability selection, the field would need to have overlooked as much as 50% genotype-dependant mortality (or infertility) for each sex every generation, which seems implausible in these taxa.

Greater divergence can be generated across a broader range of selection values when an antagonistic locus transiently sweeps through a population. Here a viability cost of 10% produces higher divergence than at equilibrium, although divergence is still low in absolute terms ($F_{ST} < 0.002$ across dominance values, under random mating). Again, at least a 30% viability cost would be required to produce F_{ST} values above 0.05. Sex-specific beneficial dominance ($h_m = 0$, $h_f = 0$) is expected to generate the lowest levels of between-sex divergence, while sex-specific deleterious dominance ($h_m = 1$, $h_f = 1$) yields the greatest levels divergence, though such a scenario seems biologically unstable (Fig. 4B). Importantly, under weak selection dominance has only a negligible effect on divergence. In fact, varying dominance does not generate quantitative changes in F_{ST} unless selection is remarkably strong ($s > 0.5$). Rather, asymmetry in selection is a critical driver of divergence in non-equilibrium populations, as this asymmetry is precisely the factor that moves populations away from equilibrium conditions to a state in which the least costly allele sweeps to fixation (Fig. 4C). Across the range of α values, divergence increases as selection differences become more extreme between the sexes. However, substantial divergence between the sexes still requires strong, asymmetric selection in non-equilibrium populations.

Sexual antagonism generates a substantial genetic load

Since male and female fitness are each maximal under fixation for different alleles at an antagonistic locus, sexually antagonistic selection generates a genetic load within the population at both a polymorphic equilibrium and during a selective sweep. At equilibrium under random mating, the load is maximized if the strengths of selection in each sex are equal (Fig. 5A), and dominance has little to no effect. Importantly, across strengths of selection up to $s = 0.5$, the load generated at equilibrium exceeds F_{ST} between males and females by nearly a factor of 10 (Fig. 5B). For example, a 10% viability cost ($s = 0.1$) results in a reduction of population fitness up to 5%, with a maximum F_{ST} value of 0.0007. The load produced by a single antagonistic locus with F_{ST} equal to the **mean** male-female F_{ST} reported in humans would exceed 20% (Fig. 5B). This relationship indicates that even weak selection driving low – and probably undetectable – levels of divergence can generate a substantial fitness reduction due to the sex-specific nature of selection.

An alternative way to examine load is by quantifying the loss of heterozygosity due to sexually antagonistic selection, using the F_{IS} statistic (the inbreeding coefficient). Under weak selection, these departures from

Hardy-Weinberg equilibrium are of similar magnitude as male-female F_{ST} (Fig. 5C). However, under strong sexual antagonism – such as that required to generate the empirically observed divergence values – F_{IS} can approach 10%.

Antagonistic loci that do not have a polymorphic equilibrium tend to produce even greater load while sweeping. Unless selection was very weak ($s < 0.05$), load tends to exceeded 10%. Under strong, asymmetric selection it can approach 70% during a sweep. Additionally, the fitness cost of sexual antagonism remains after an allele fixes. The load generated during a sweep is affected by dominance, with additive loci generating loads that are intermediate to the other dominance scenarios. Beneficial dominance within each sex can apparently resolve some of the underlying antagonism by shielding selection on heterozygotes and therefore reducing the load. In contrast, sex-specific deleterious dominance generated the greatest load.

Genome-wide antagonistic selection also produces low divergence

Our analytical results are based on a single-locus model, yet empirical studies report averages across large numbers of loci. To complement the single-locus theory, we quantified the effects of sexually antagonistic selection throughout the genome using individual-based simulations in SLiM Haller and Messer [2019]. Simulations in which every new mutation was sexually antagonistic in a population of 10,000 individuals resulted in a mean male-female F_{ST} of 0.00005 and a between-replicate standard deviation of 0.0001, consistent with the single-locus theory (since s was around 0.01). However, entirely neutral simulations (equal mutation rates but no selection) resulted in the same mean and SD of male-female F_{ST} values. Although qualitatively similar, the distribution of male-female F_{ST} values across loci was statistically significantly different between the neutral and sexually antagonistic scenarios (Kolmogorov-Smirnov test: $D = 0.09$, $p < 0.001$; Fig. 6A). However, this difference in distributions is driven by the larger number of intermediate frequency alleles in the sexually antagonistic scenario. In particular, neutral simulations had no SNPs with a frequency above 10%, while sexually antagonistic simulations had over 1,000 SNPs with a frequency above 10%. Despite there being true differences between the neutral and sexually antagonistic scenarios, the male-female divergences observed were still exceptionally low. In fact, neither model had any loci with male-female F_{ST} greater than 0.0012 (Fig. 6A). Sexually antagonistic simulations had an average 22% decrease in population fitness ($L = 0.22 \pm 0.03$) after 1000 generations of evolution, again consistent with single-locus calculations. Even the minimum load observed under the sexually antagonistic scenario corresponded to a 16% decrease in population fitness.

Sampling variance can generate spurious signals of male-female divergence

Both the single locus model and genome-wide simulations indicate that, while theoretically possible, we would need strong sexually antagonistic viability selection to maintain high divergence between the sexes. Alternatively, the large observed F_{ST} statistics might be due to sampling variance. The empirical studies we cite have relatively small sample sizes (N = 15-200). The male-female F_{ST} values we reported above from simulation were calculated from the *entire* population. To evaluate the effect of sampling, we calculated male-female F_{ST} values from random samples of individuals in our SLiM simulations of two sizes: 100 individuals (50 females and 50 males) and 50 individuals (25 females and 25 males). This subsampling produced dramatically higher male-female F_{ST} values under both the neutral (100 individuals, mean $\pm$ standard deviation across replicates: $F_{ST} = 0.005 \pm 0.005$; 50 individuals: $F_{ST} = 0.01 \pm 0.007$) and sexually antagonistic (100 individuals: $F_{ST} = 0.005 \pm 0.004$; 50 individuals: $F_{ST} = 0.01 \pm 0.009$) simulations (Fig. 6B). There was a significant difference in the distribution of male-female F_{ST} values between the neutral and sexually antagonistic simulations both when subsampling at 100 individuals (Kolmogorov-Smirnov test: $D = 0.067$, $p < 0.001$) and 50 individuals ($D = 0.096$, $p < 0.001$). However, there was no correlation between the F_{ST} values calculated from the full population and those obtained from samples of either 100 individuals ($r = 0.016$) or the 50 individual subset ($r = -0.010$). This lack of correlation also holds true for the neutral model (100 individuals: $r = 0.025$; 50 individuals: $r = -0.011$).

Although there are more high male-female F_{ST} sites in samples from the sexually antagonistic simulations (Fig. 6B), this does not seem to be a direct result of selection, but rather a due to the fact that there are

many more intermediate frequency alleles in the sexually antagonistic simulations due to balanced polymorphisms. To test this, we calculated F_{ST} between two random samples of size 50 drawn from each simulation *independently* of sex, and also between random samples of size 25. If the enrichment of high between-sex F_{ST} sites in the antagonistic simulations are in fact due to the difference in allele frequency distribution rather than the direct result of selection, then the enrichment should persist even in these samples drawn after randomizing sex. Indeed this enrichment persists, as shown in Fig. 6C. Thus, the higher number of intermediate frequency sites in the sexually antagonistic model creates a higher sampling variance of F_{ST}, as expected based on theory [Jakobsson et al., 2013]. In particular, the tail of the F_{ST} distributions show many higher values, such that an increase by two orders of magnitude relative to the full population was observed (Fig. 6B). These results suggest that separating signals of weak antagonistic selection from sampling noise will be extremely difficult.

Discussion

Sexually antagonistic viability selection creates allelic divergence between the sexes because the proportions of each genotype that die before reproduction differs between the sexes. This between-sex divergence for non-sex-linked elements is created anew each generation because chromosomal segregation re-assorts autosomal associations across sexes during sexual reproduction. However, discussions of sexually antagonistic pleiotropy have often not focused on the effects of transmission on locus dynamics [Rice and Holland, 1997]. An emerging trend in sexual antagonism research is the use of male-female genomic comparisons to identify sexually antagonistic loci. These recent studies identified hundreds to thousands of sexually divergent autosomal loci with mean divergence between the sexes in the range of 2-7%. Taken as reported, these studies suggest the extent and strength of sexually antagonistic selection is far greater than might be anticipated. To assess these claims, we used a population genetic model to determine the magnitude of divergence generated by sexually antagonistic viability selection, the strength of selection required to drive such divergence, and the population fitness costs generated by this process.

Although sexual antagonism has been a topic of particular interest over the last few decades [Arnqvist and Rowe, 2005], some of the early investigations of sex-specific selection were largely motivated as part of a general attempt to elucidate all possible means by which the large amounts of segregating polymorphisms observed within natural populations could be maintained [Lewontin, 1974]. In this context, Kidwell et al. [1977] showed that strong sex-specific selection ($s > 0.5$) could maintain a polymorphism at an autosomal locus when alleles had opposing effects in the sexes. Our analysis agrees with Kidwell et al. [1977], but we find that maintainence of such polymorphisms would create a substantial genetic load. Additionally, with weaker selection, the parameter space allowing a stable polymorphism becomes quite narrow. This difference highlights the necessity for considering biologically relevant conditions – as similarly discussed by Smith and Hoekstra [1980] – particularly when theory is is informing signatures of selection within the genome. An important contribution of this model is the explicit inclusion of transmission, which allows for non-random mate choice – a potentially important underlying component of sexual conflict [Arnqvist and Rowe, 2005] – to be considered. Assortative mating can indeed have a large impact on the conditions for the maintenance of polymorphism. Supporting previous simulations [Arnqvist, 2011], we found positive assortative mating by fitness maintained polymorphisms. In particular, the combination of asymmetrical selection between the sexes and deleterious dominance conditions expanded the equilibrium space relative to random mating. However, such deleterious sex-specific dominance would likely be selected against, suggesting that the strength of selection is the more relevant parameter in natural populations.

While the maintenance of polymorphism may have been a primary motivation for previous work, a goal of modern genomics is to use specific signals of genomic differentiation to identify the loci underlying sexually antagonistic genetic effects [Mank, 2017b, Kasimatis et al., 2017]. Building on our previous work [Kasimatis et al., 2017] allowed us to consider the expected degree of between-sex divergence both when an antagonistic polymorphism is maintained at equilibrium in the population, and when no such stable equilibrium exists, so one of the two alleles sweeps towards fixation to the detriment of one sex. Our model and accompanying simulations highlight several potential limitations of detecting sex-specific differentiation in empirical studies.

First, detectable quantitative divergence between the sexes requires exceptionally strong sexually antagonistic selection. Even a 10% viability cost in each sex resulted in between-sex F_{ST} values of less than 0.001 (Fig. 4), a signal that is unlikely to be distinguishable from noise without sampling many thousands of individuals within each sex. Critically, the mean divergence measured in several empirical datasets – including humans – would require a 30% to 60% viability cost in each sex under our model. These remarkably high sex-specific mortality rates are, to the best of our knowledge, not observed in nature [see Singh and Punzalan, 2018] and would presumably be fairly evident in observations of within-generation population biology. (However, exceptionally high fecundity animals might withstand such high sex-specific mortality [see Williams, 1975].) Strong sex-specific gametic selection is more plausible than viability selection on adults, but such high levels of genotype-dependent gamete "mortality" in these organisms still do not seem consistent with empirical observations.

Second, asymmetry in the strength of selection between the sexes is critical in determining the degree of divergence generated. When the strength of selection is weak and approximately the same between the sexes, polymorphisms may be stably maintained, but between-sex divergence is small. However, there is no *a priori* reason to expect that antagonistic mutations should be perfectly symmetrical in their effects and therefore that polymorphic loci should be stable over time. Alleles with more asymmetric effects will often sweep, producing larger but transient between-sex divergences, although again only under moderate to strong selection. Here, we found that dominance has little quantitative effect on male-female divergence, particularly when selection is weak. In general, understanding what the distribution of sex-specific effects underlying antagonistic selection looks like will provide important information on the potential for sexually antagonistic loci to contribute to genetic variation and genome evolution.

Third, regardless of the allele-frequency dynamics, the genetic load created by sexually antagonistic selection is substantial. Even weak selection generates a measurable decrease in population mean fitness. Interestingly, sex-specific beneficial dominance can mitigate load to some extent and potentially provides an opportunity for alleles that modify these dominance relationships to invade. This overdominance-like scenario would be expected to generate a form of cryptic genomic conflict and could potentially lead to the persistence of antagonism. Overall, however, our single locus results indicate that male-female allelic divergence is extremely difficult to generate and that the fitness costs of unresolved antagonism are considerable.

Thus, the theoretical predictions from our single locus model seem at odds with the empirical patterns reported to date. Taken as true measurements of sexually antagonistic selection, the empirical data could be described by two, non-exclusive genomic patterns. Divergent loci could either be stable polymorphisms or could be arising and sweeping to fixation through a constant genomic churn of antagonistic interactions. Our results show that either of these explanations require an exceptionally high genetic load. Again, there is currently no indication that mortality occurs in such a high, sex-specific manner, particularly in some of the vertebrate species that have been examined.

Individual-based simulations with many linked selected loci genome-wide recapitulate the predictions of the single-locus model, finding again that even in this more complex situation, weak selection can only produce very low levels of divergence. Most importantly, however, we found that estimating male-female F_{ST} from samples of the sizes used in the literature (hundreds or less) produced distributions with larger means and longer tails, even in the complete absence of antagonistic selection. Even in simulations with antagonistic selection, any high divergence values were a result of random sampling noise, and did not correlate with the true divergence values or strength of selection. These simulations highlight the sensitivity of F_{ST} statistics to sampling variance, which is a major obstacle for identification of antagonistic loci from sex-specific differentiation. Most existing empirical studies have not taken these effects fully into account. Our simulations are not intended to be comprehensive, but demonstrate that sampling variance can be more important than selection itself in driving high estimates of divergence, and highlight the need for proper sampling theory.

At the very least, studies reporting high male-female F_{ST} values should compare these values to empirical distributions found by random permutation of sex labels, as done by Dutoit et al. [2018]. However, population substructure may remain a concern, since such a permutation test does not account for cryptic correlations with sex. For instance, suppose that the sampled population is composed of a mixture of two diverged

subpopulations, and that the sex and admixture coefficients of the sampled individuals are correlated. (The samples in Dutoit et al. [2018] were all taken from a single island, so this seems unlikely to explain their results.) Other estimation issues beyond sampling variance may well play a role in the large observed male-female F_{ST} values. Reads from the sex chromosomethat are wrongly aligned to an autosome, particularly in the heterogametic sex, have the potential to generate spurious F_{ST} peaks, an issue that may affect some classes of genes – such as those with sex-biased expression – more than others. Furthermore, existing studies report large numbers of loci with high average F_{ST}. Should we interpret this as evidence of antagonistic selection across many loci simultaneously, or at just one a few loci that affect others through linkage? This is not clear, because each generation's sex-specific selection on a single antagonistic allele will also cause between-sex frequency differences at other loci to the extent they are in linkage disequilibrium with the locus under selection. More work is needed to quantify this effect so that they can be included in analyses of natural populations.

Rather, many of the loci currently identified as being caused by sex-specific antagonistic selection seem likely to be spurious signals resulting from poor statistical inference. While we believe sexually antagonistic selection does contribute to genomic evolution, we strongly caution against the use and over-interpretation of male-female F_{ST} statistics until better sampling theory is developed.

Acknowledgements:

We thank Göran Arnqvist and Thomas Nelson for their helpful discussion. This work was supported by the National Institutes of Health (training grant T32GM007413 to KRK and R01GM102511 to PCP) and the ARCS Oregon Chapter (KRK).

References

G Arnqvist. Assortative mating by fitness and sexually antagonistic genetic variation. *Evolution*, 65(7): 2111–2116, July 2011.

G Arnqvist and L Rowe. *Sexual conflict*. Princeton University Press, 2005.

W F Bodmer. Differential Fertility in Population Genetics Models. *Genetics*, 51(3):411–424, March 1965.

R Bonduriansky and S F Chenoweth. Intralocus sexual conflict. *Trends in Ecology & Evolution*, pages 1–9, March 2009.

D Charlesworth and B Charlesworth. Sex differences in fitness and selection for centric fusions between sex-chromosomes and autosomes. *Genetical research*, 35(2):205–214, April 1980.

C Cheng and M Kirkpatrick. Sex-Specific Selection and Sex-Biased Gene Expression in Humans and Flies. *PLoS Genetics*, 12(9):e1006170–18, September 2016.

T Connallon and A G Clark. The Resolution of Sexual Antagonism by Gene Duplication. *Genetics*, 187(3): 919–937, March 2011.

T Connallon, R M Cox, and R Calsbeek. Fitness consequences of sex-specific selection. *Evolution*, 64(6): 1671–1682, June 2010.

L Dutoit, C F Mugal, P Bolívar, M Wang, K Nadachowska-Brzyska, L Smeds, H Papoli, L Gustafsson, and H Ellegren. Sex-biased gene expression, sexual antagonism and levels of genetic diversity in the collared flycatcher (ficedula albicollis) genome. *Molecular Ecology*, pages 1–31, July 2018.

S P Flanagan and A G Jones. Genome-wide selection components analysis in a fish with male pregnancy. *Evolution*, 71(4):1096–1105, April 2017.

J D Fry. The genomic location of sexually antagonistic variation: some cautionary comments. *Evolution*, 64 (5):1510–1516, May 2010.

J B S Haldane. The effect of variation of fitness. *American Naturalist*, 71(735):337–349, 1937.

J B S Haldane. The cost of natural selection. *Journal of Genetics*, 55(3):511–524, December 1957.

Benjamin C Haller and Philipp W Messer. SLiM 3: Forward Genetic Simulations Beyond the Wright-Fisher Model. *Molecular Biology and Evolution*, 36(3):632–637, March 2019.

S Immler and Sarah P Otto. The Evolutionary Consequences of Selection at the Haploid Gametic Stage. *The American Naturalist*, 192(2):241–249, August 2018.

John Jaenike. Sex Chromosome Meiotic Drive. *dx.doi.org*, 32(1):25–49, November 2003.

Mattias Jakobsson, Michael D Edge, and Noah A Rosenberg. The Relationship Between FST and the Frequency of the Most Frequent Allele. *Genetics*, 193(2):515–528, February 2013.

S Joseph and M Kirkpatrick. Haploid selection in animals. *Trends in Ecology & Evolution*, 19(11):592–597, November 2004.

K R Kasimatis, T C Nelson, and P C Phillips. Genomic signatures of sexual conflict. *The Journal of heredity*, 108(7):780–790, October 2017.

J F Kidwell, M T Clegg, F M Stewart, and T Prout. Regions of stable equilibria for models of differential selection in the two sexes under random mating. *Genetics*, 85(1):171–183, January 1977.

M Kozielska, F J Weissing, L W Beukeboom, and I Pen. Segregation distortion and the evolution of sex-determining mechanisms. *Heredity*, 104(1):100–112, January 2010.

R C Lewontin. The genetic basis of evolutionary change. Columbia University Press, New York, 1974.

E A Lucotte, R Laurent, E Heyer, L Ségurel, and B Toupance. Detection of Allelic Frequency Differences between the Sexes in Humans: A Signature of Sexually Antagonistic Selection. *Genome Biology and Evolution*, 8(5):1489–1500, June 2016.

J E Mank. The transcriptional architecture of phenotypic dimorphism. *Nature Publishing Group*, 1(1):1–7, January 2017a.

J E Mank. Population genetics of sexual conflict in the genomic era. *Nature Reviews Genetics*, 7:1–10, October 2017b.

M M Patten and D Haig. Maintenance or loss of genetic variation under sexual and parental antagonism at a sex-linked locus. *Evolution*, 63(11):2888–2895, November 2009.

R Core Team. *R: A Language and Environment for Statistical Computing*. R Foundation for Statistical Computing, Vienna, Austria, 2018. URL `https://www.R-project.org/`.

W R Rice. Sex chromosomes and the evolution of sexual dimorphism. *Evolution*, 38(4):735, 1984.

W R Rice. The accumulation of sexually antagonistic genes as a selective agent promoting the evolution of reduced recombination between primitive sex chromosomes. *Evolution*, 41(4):911–914, July 1987.

W R Rice and B Holland. The enemies within: intergenomic conflict, interlocus contest evolution (ICE), and the intraspecific Red Queen. *Behavioral Ecology and Sociobiology*, 41(1):1–10, 1997.

A Singh and D Punzalan. The strength of sex-specific selection in the wild. *Evolution*, October 2018.

John Maynard Smith and R Hoekstra. Polymorphism in a varied environment: how robust are the models? *Genetics Research*, 35(1):45–57, February 1980.

G C Williams. *Sex and evolution.* Princeton University Press, Princeton, NJ, 1975.

A E Wright, M Fumagalli, C R Cooney, N I Bloch, F G Vieira, S D Buechel, , N Kolm, and J E Mank. Male-biased gene expression resolves sexual conflict through the evolution of sex-specific genetic architecture. *Evolution Letters*, 215:403–10, February 2018.

S Wright. The genetical structure of populations. *Annals of eugenics*, 15(4):323–354, March 1951.

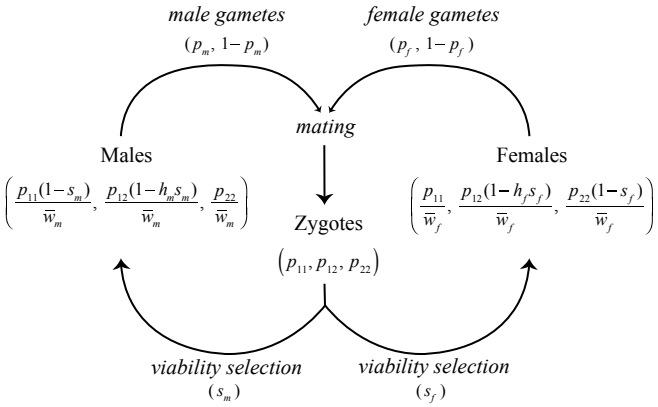

Figure 1: Lifecycle of the model. Zygotes are subject to sexually antagonistic viability selection (s_m and s_f), perturbing allele frequencies in adults in a sex-specific manner. Sex-specific adult allele frequencies are given in Equations 1 and 2, where $\bar{w}_f = \mathbf{w_f} \cdot \mathbf{p_t}$ and $\bar{w}_m = \mathbf{w_m} \cdot \mathbf{p_t}$. Surviving adults produce gametes of each allele type in frequencies corresponding to Equations 1 and 2. At this time meiotic segregation breaks the association between the locus and sex. Females and males mate with frequencies proportional to the mate choice matrix ($\mathbf{M}$) to produce the zygote pool in the next generation. Kidwell et al. [1977] gives the recursion for the allele frequencies in gametes (p_m, p_f), under the assumption of random, genotype-independent mating.

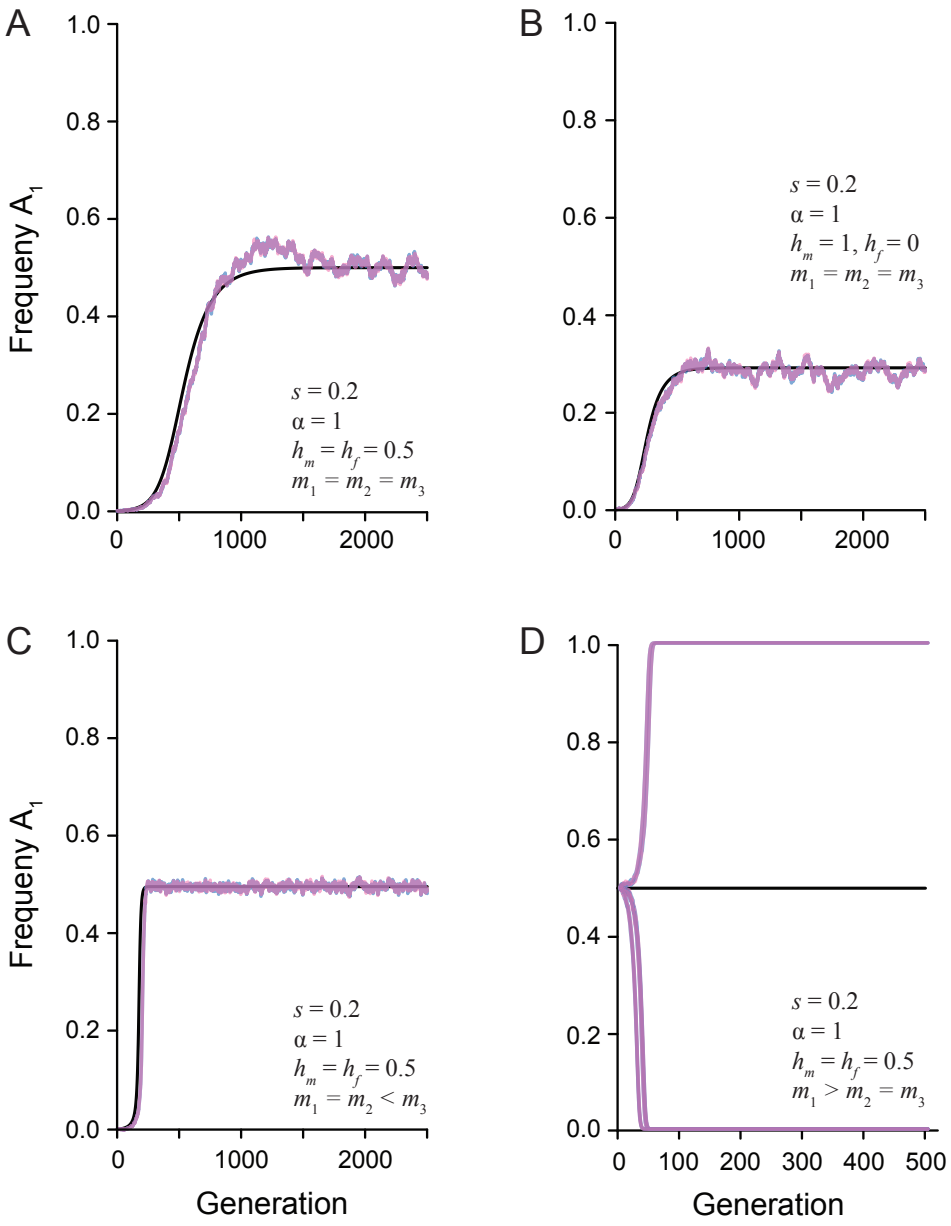

Figure 2: The change in the frequency of a newly derived sexually antagonistic allele (A_1) over time. The black line represents the predicted allele frequency from the recursion equation. The overlaid pink and blue lines represent the simulated population (N = 20,000) of females and males, respectively. The strength of selection (s), ratio of selection between the sexes (α), dominance relationship (h_m and h_f), and mate choice coefficients (m_1, m_2, and m_3) are given in each panel. A) Random mating with additive dominance and symmetric selection between the sexes maintains a stable polymorphism. B) Random mating with complete male dominance and symmetric selection between the sexes maintains a stable polymorphism. C) Assortative mating by fitness with additive dominance maintain a stable polymorphism. D) Assortative mating by genotype with additive dominance has an unstable equilibrium. Multiple simulated populations show how drift will quickly lead to fixation or loss of the A_1 allele.

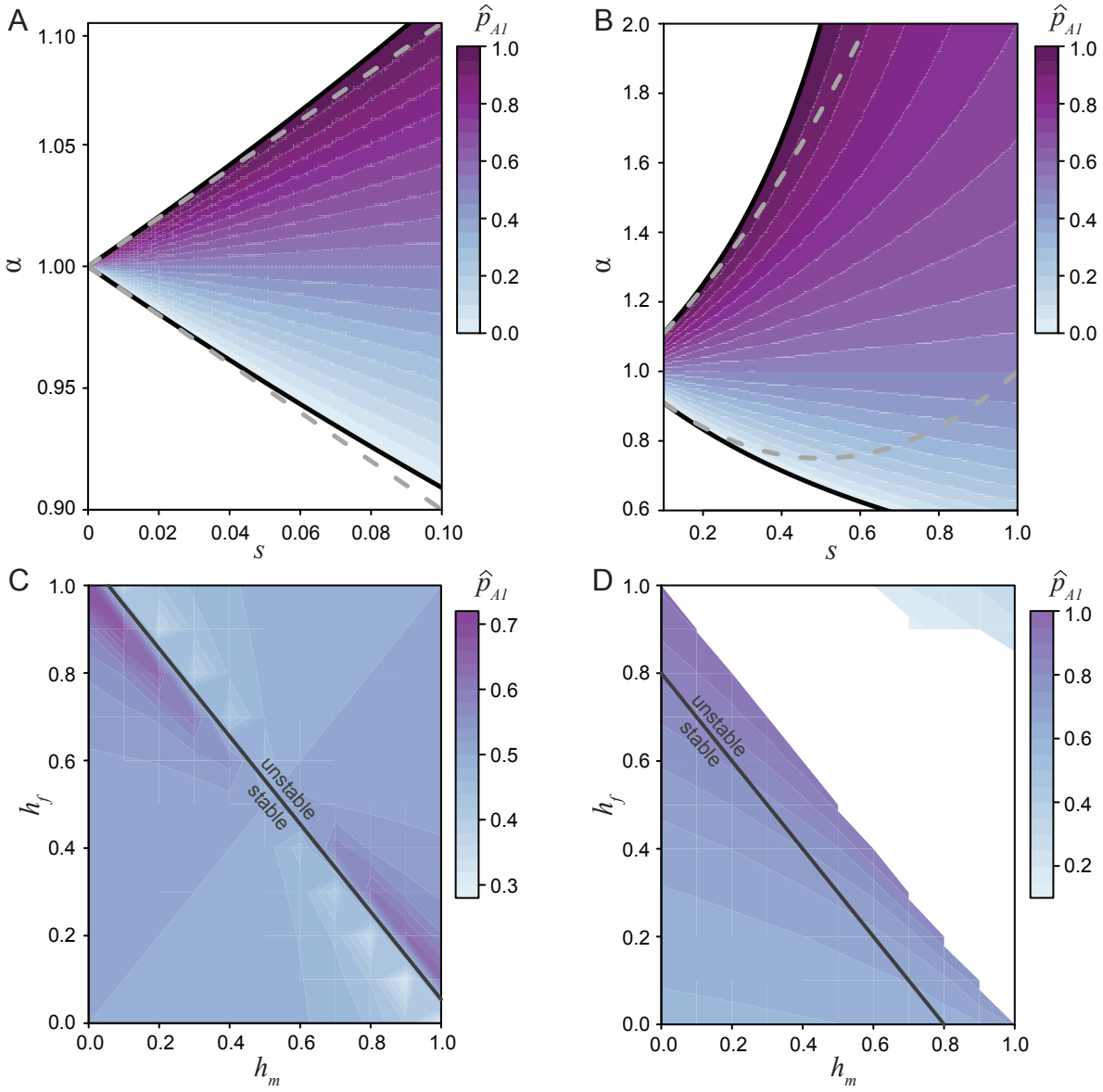

Figure 3: The equilibrium space for the A_1 allele under differing selection and dominance conditions. A) The equilibrium space at an additive locus ($\hat{p}_{A1}$, Equation 10), when selection is weak and related between the sexes by the ratio α. Here the equilibrium space is symmetric around $\alpha = 1$ and confined to approximately equal selection between the sexes. The solid black line represent the permissible bounds on α (7) and the dashed gray line represents the first order Taylor series approximation. B) The equilibrium space at an additive locus increases as the strength of selection increases. The solid black line represents the bounds on α and the dashed gray line represents the second order Taylor series approximation. C) The equilibrium space across all dominance conditions when selection is equal between the sexes ($s = 0.1, \alpha = 1$). When the dominance coefficients between the sexes sum to no greater than one ($h_m + h_f \leq 1$), then the equilibrium is stable. However, when the sum is greater than one the equilibrium is unstable. D) Strong, asymmetric selection ($s = 0.4, \alpha = 1.5$) narrows the equilibrium space and range of stable conditions ($h_m + h_f \leq 0.8$).

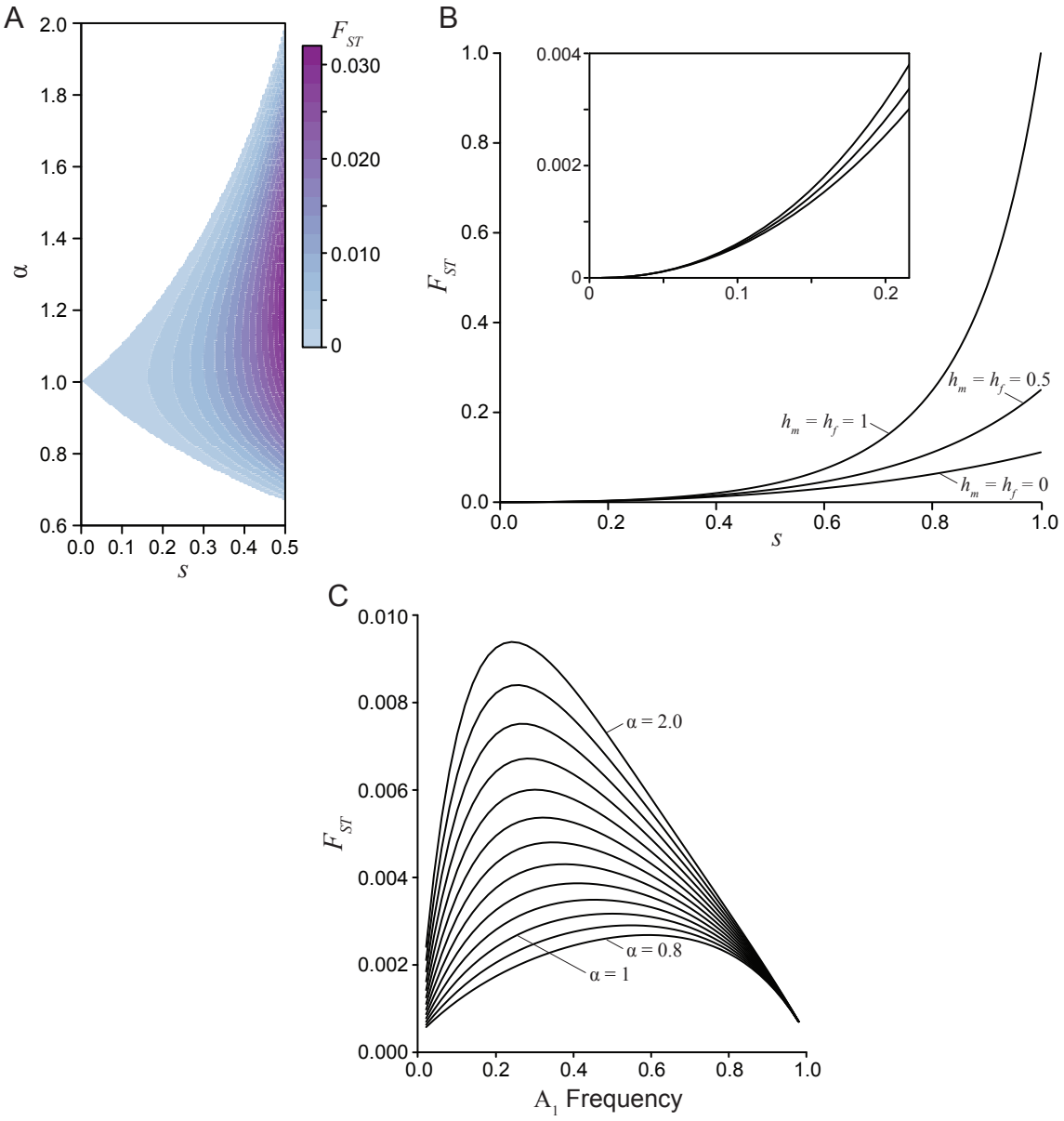

Figure 4: Divergence between the sexes due to a single generation of sexually antagonistic selection. A) Male-female F_{ST} for an additive locus ($h_m = h_f = 0.5$) at equilibrium, where the strength of selection between the sexes is related by the ratio α. B) Male-female F_{ST} as a function of selection for three dominance regimes: sex-specific beneficial ($h_m = h_f = 0$), additive ($h_m = h_f = 0.5$), and deleterious ($h_m = h_f = 1$). Sex-specific beneficial dominance always results in the lowest divergence between the sexes. The inset graph highlights the similarly low divergence values generated under weak and moderately weak selection. C) Male-female F_{ST} at a sex-beneficial locus ($h_m = h_f = 0$) as a function of A_1 allele frequency for varying degrees of asymmetry in selection ($s = 0.2$ and $0.8 \leq \alpha \leq 2$).

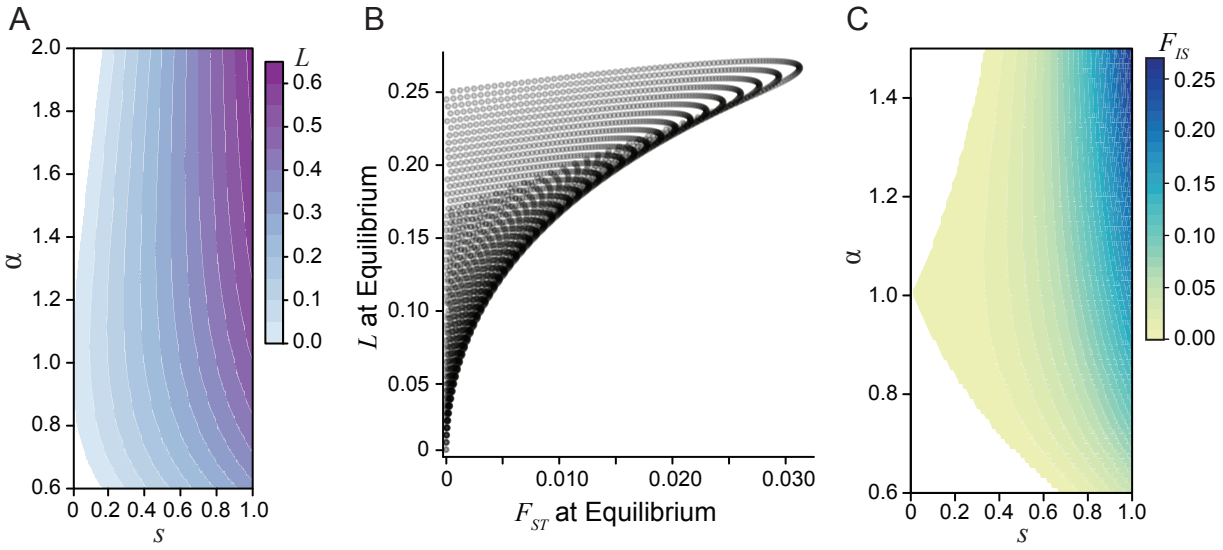

Figure 5: The genetic load created by sexually antagonistic selection. A) The genetic load generated at equilibrium for an additive locus across strengths (s) and asymmetries (α) of selection. B) A comparison of male-female divergence and genetic load for a locus at equilibrium across a gradient of selection coefficients with varying asymmetry. The load generated at a locus exceeds the degree of divergence between the sexes. Each curve corresponds to a different fixed strength of selection from $s = 0$ to $s = 0.5$ and each point along the curves corresponds to a different value of α from 0.6 to 2. C) The population inbreeding coefficient F_{IS} for an additive locus ($h_m = h_f = 0.5$) at equilibrium. The excess of homozygous individuals represents the departures from Hardy-Weinberg equilibrium due to sex-specific selection.

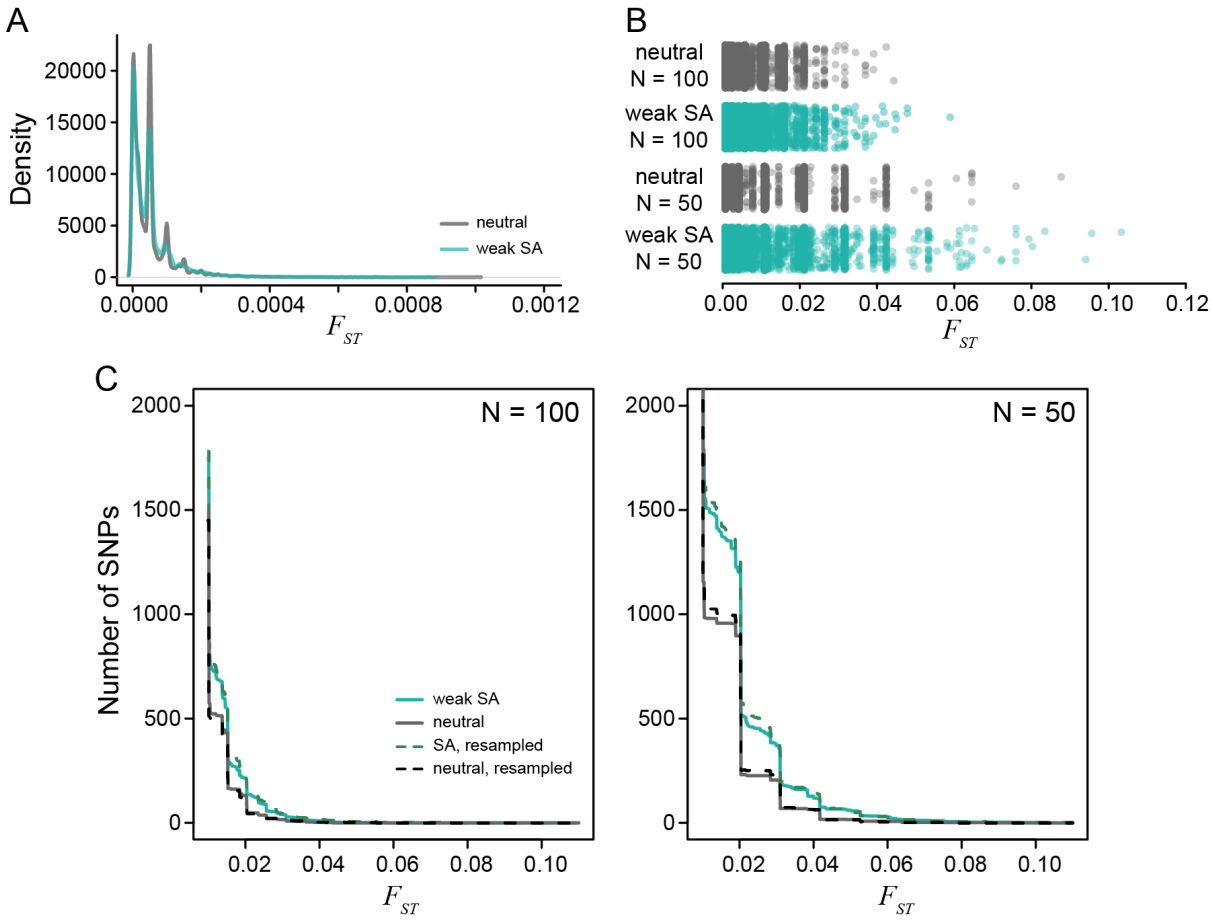

Figure 6: The distribution of per locus F_{ST} values generated from simulated populations after 1000 generations of evolution. A) The density of male-female F_{ST} values for a population of 10,000 individuals is centered around $F_{ST} = 0.0005$. The neutral (gray) and sexually antagonistic (teal) scenarios were similar but statistically significantly different. B) The distribution of male-female F_{ST} values when subsampling the full populations to either 100 individuals or 50 individuals with equal sex ratios. The sexually antagonistic scenario is significantly different from the neutral scenario due to an increased sampling variance in the sexually antagonistic scenario. C) Cumulative distribution curves of per-locus male-female F_{ST} values, both between random samples from the two sexes (solid lines) and between sets of individuals chosen randomly independently of sex (dotted lines). Male-female F_{ST} distributions differed between neutral (grey) and antagonstic (teal) simulations but were not higher for between-sex comparisons, showing that higher F_{ST} values in the antagonistic simulation was not directly due to selection.